Int J Theor Phys (2008) 47: 2971–2990
DOI 10.1007/s10773-008-9732-z

Entropy Growth and Degradation of Entanglement Due to Intrinsic Decoherence for an Initial Mixed State in the Multi-Quanta JC Model

H.A. Hessian

Received: 16 November 2007 / Accepted: 28 March 2008 / Published online: 10 April 2008

Abstract In this paper, we present a study of the entropy growth and degradation of entanglement due to intrinsic decoherence for some different initial states in the multi-quanta Jaynes-Cummings model. We analytically solve the Milburn equation for such JC model. Using an established entanglement measure based on the negativity of the eigenvalues of the partially transposed density matrix we find a very strong sensitivity of the maximally generated entanglement to the amount of decoherence, the multiplicity and the form of the and the initial state. Comparison with different measures of entanglement are made.

Keywords Entanglement · Entropies · Negativity · Mixed state · Intrinsic decoherence

1 Introduction

The quantum entanglement has become a subject for intensive study among those interest in the foundations of quantum theory. But more recently (starting less than ten years ago), entanglement has come to be viewed not just as a tool for exposing the weirdness of quantum mechanics, but as a potentially valuable resource. By exploiting entangled quantum states, we can perform tasks that are otherwise difficult or impossible. Recently much attention has been focused on the entanglement of the field and atom in the Jaynes-Cummings (JC) model [1–13]. The authors in [1–4] have shown that entropy is a very useful operational measure of the entanglement degree of the quantum state, which automatically includes all moments of the density operator. The time evolution of the field (atomic) entropy reflects the time evolution of the degree of entanglement between the particle and the field. The higher the entropy, the greater the entanglement. On the other hand, ion trap quantum computation, first introduced by Cirac and Zoller [14], is a potentially powerful technique for the storage and manipulation of quantum information. Recently, much progress has been made in the preparation, manipulation and measurement of quantum states of the center-of-mass vibrational motion of a single atom experimentally [15–22] and theoretically [14, 23–37], which

H.A. Hessian (✉)
Faculty of Science, Assiut University, Assiut, Egypt
e-mail: ammar_67@yahoo.com

are not only of fundamental physical interest but also of practical use for sensitive detection of week signals [38, 39] and quantum computation [14, 15].

Models have been constructed to describe a two-level ion undergoing quantized vibrational motion within a harmonic trapping potential and interacting with a classical light field [40–45]. It has been pointed out that the dynamics of a trapped ion can be described by a Hamiltonian similar to a JC model [46] or its generalizations under certain regimes [24, 25, 33–35, 37, 47, 48]. Despite these heroic experimental achievements, the quantum motion of a single atom is obviously limited by sources of decoherence. Decoherence arises from random and unknown perturbations of the Hamiltonian. If these perturbations cannot be followed exactly, experiments must average over them. This leads to an effective irreversible evolution of the atom and a suppression of coherent quantum features through the decay of off-diagonal matrix elements of the density operator in some basis. Complementary to the decay of off-diagonal matrix elements, noise is added to conjugate variables. This can appear as a heating of the atom if noise is added to the momentum variable. On the other hand, there has been increased interest in the decoherence problem in quantum mechanics because of its possible application in quantum measurement processes and quantum computers [49, 50].

The intrinsic decoherence approach has been proposed and investigated in the framework of several models [51–57]. In particular, Milburn [58, 59] proposed a simple intrinsic decoherence models based on an assumption that on sufficiently short time steps the system evolves in a stochastic sequence of identical unitary transformations. This assumption modifies the von Neumann equation for the density operator of a quantum system through a simple modification of the usual Schrödinger evolution equation. The off-diagonal elements of the density operator in Milburn's model are intrinsically suppressed in the energy eigenstate basis, thereby intrinsic decoherence is realized without the usual dissipation associated with the normal decay. The decay is entirely of phase dependence only. Free evolution of a given quantum system has been discussed early [58, 59] but investigations of interacting sub-systems followed [60–66].

Decoherence due to normal decay is often said to be the most efficient effect in physics, to a point where observation comes too late after the effect has reached completion [67]. The effect in action has been observed in quantum optics where the decoherence phenomena transforming a Schrödinger-cat into a statistical mixture was observed while unfolding [68]. There has been considerable interest in the properties of the so-called superposition states of light (*SS*) involving superpositions of coherent states with strongly differing amplitude [69–75]. One particularly interesting case is the superposition of two coherent states of fixed amplitude but opposite phase [70–75]. Due to the quantum interference, the properties of such a superposition are very different from the properties of the constituent states (coherent states), as well as from the incoherent superposition or statistical mixture (*SM*) of coherent states.

In this paper, we aim at extending the previously cited treatment to study the entropy growth and degradation of entanglement due to intrinsic decoherence for some different initial states in the multi-quanta JC model. We will obtain an exact solution of the Milburn equation for the multi-quanta JC model. We use this solution to study the degradation of entanglement and entropy growth due to the intrinsic decoherence for the superposition states of light (*SS*) and statistical mixture state (*SM*). Finally conclusion are provided. This paper is organized as follows: In Sect. 2, we obtain an exact solution of the Milburn equation for the multi-quanta JC model and give the explicit expression of this solution in the two-dimensional basis of the particle. Sections 3 and 4 are devoted to an investigation the degradation of entanglement and entropy growth due to the intrinsic decoherence for the

multi-quanta JC model in the resonant or the off-resonant cases. Finally, some concluding remarks are provided.

2 Exact Solution of the Milburn Equation

We consider a quantum system described by the density operator $\rho(t)$. In standard quantum mechanics, dynamics of the system is governed by the evolution operator $\hat{U}(t) = \exp[-\frac{i}{\hbar}t\hat{H}]$, where $\hat{H}$ is the Hamiltonian describing the system. Milburn assumed [58, 59] that on sufficiently short time steps the system does not evolve continuously under unitary evolution but rather in a stochastic sequence of identical unitary transformation. Based on this assumption, he has derived the equation for the time evolution density operator $\rho(t)$ of the quantum system [58, 59]

$$\frac{d}{dt}\hat{\rho}(t) = \gamma\left\{\exp\left[-\frac{i}{\hbar\gamma}\hat{H}\right]\hat{\rho}(t)\exp\left[\frac{i}{\hbar\gamma}\hat{H}\right] - \hat{\rho}(t)\right\}, \tag{1}$$

where γ is the mean frequency of the unitary time step. This equation formally corresponds to the assumption that on sufficiently short time steps the system evolves with a probability $p(\tau) = \gamma\tau$. Obviously, the generalized (1) alters the Schrödinger dynamics. It reduces to the ordinary von Neuman equation for the density operator in the limit $\gamma \to +\infty$. Expanding (1) to first order in γ^{-1}, the following dynamical equation is obtained:

$$\frac{d}{dt}\hat{\rho}(t) = -\frac{i}{\hbar}[\hat{H}, \hat{\rho}] - \frac{1}{2\hbar^2\gamma}[\hat{H}, [\hat{H}, \hat{\rho}]] \tag{2}$$

which is the Milburn equation that we shall study below. This equation has been solved for a harmonic oscillator and a precessing spin system [58, 59] the simple JC model [60–62], the resonant multiphoton JC model [63] and the nondegenerate two-mode JC model [64–66]. In what follows we shall consider the exact solution of this equation for multi-quanta JC model with a detuning parameter in either a superposition state (*SS*) or a mixture state (*SM*).

The system considered here consists of a two-level particle (atom or trapped ion) interacting with a single-mode quantized field via m-quanta transition processes, where m is the multiplicity such a generalization is of considerable interest because of its relevance to study of the coupling between a single atom and the radiation field with the atom making m-quanta transitions. The Hamiltonian in the rotating wave approximation (RWA) [46–48, 76–78], is written as:

$$\hat{H} = \omega\hat{a}^\dagger\hat{a} + \frac{\omega_\circ}{2}\hat{\sigma}_z + \lambda(\hat{a}^{\dagger m}\hat{\sigma}_- + \hat{a}^m\hat{\sigma}_+), \quad (\hbar = 1), \tag{3}$$

where ω is the field frequency and $\omega_\circ$ is the transition frequency between the excited and ground states of the particle (atom or trapped ion), $\hat{a}$ and $\hat{a}^\dagger$ are the annihilation and the creation operators of the cavity field respectively; λ is the effective coupling constant, $\hat{\sigma}_z$ is the population inversion operator, and $\hat{\sigma}_\pm$ are the "spin flip" operators which satisfy the relation $[\hat{\sigma}_+, \hat{\sigma}_-] = \hat{\sigma}_z$ and $[\hat{\sigma}_z, \hat{\sigma}_\pm] = \pm 2\hat{\sigma}_\pm$, with the detuning parameter $\Delta = \omega_\circ - m\omega$.

Now, we look for the exact solution for the density operator $\hat{\rho}(t)$ of the Milburn equation (2) taking into account the Hamiltonian (3).

For convenience, we introduce three auxiliary superoperators [60–66] $\hat{J}$, $\hat{S}$ and $\hat{L}$ defined by

$$\exp(\hat{J}\tau)\hat{\rho}(t) = \sum_{k=0}^{\infty}\frac{1}{k!}\left(\frac{\tau}{\gamma}\right)^k\hat{H}^k\hat{\rho}(t)\hat{H}^k, \tag{4}$$

$$\exp(\hat{S}\tau)\hat{\rho}(t) = \exp(-i\hat{H}\tau)\hat{\rho}(t)\exp(i\hat{H}\tau), \tag{5}$$

$$\exp(\hat{L}\tau)\hat{\rho}(t) = \exp\left[-\frac{\tau}{2\gamma}\hat{H}^2\right]\hat{\rho}(t)\exp\left[-\frac{\tau}{2\gamma}\hat{H}^2\right], \tag{6}$$

where the Hamiltonian $\hat{H}$ is given by (3).

It is straightforward to obtain the formal solution of the Milburn equation (2) as follows:

$$\hat{\rho}(t) = \exp(\hat{J}t)\exp(\hat{S}t)\exp(\hat{L}t)\hat{\rho}(0), \tag{7}$$

where $\hat{\rho}(0)$ is the density operator of the initial particle-field system.

We assume that the initial field inside the cavity is in a superposition state and the particle in its excited state $|\, e\rangle$, so that:

$$\begin{aligned}\hat{\rho}(0) = \frac{1}{L}[&|\,\alpha\rangle\langle\alpha\,| + r^2\,|\,-\alpha\rangle\langle-\alpha\,| \\ &+ r(|\,\alpha\rangle\langle-\alpha\,| + |\,-\alpha\rangle\langle\alpha\,|)]\otimes|\,e\rangle\langle e\,|,\end{aligned} \tag{8}$$

where $L = [1 + r^2 + 2r\exp(-2\alpha^2)]$, with α real. The parameter r can assume the values -1, 0 and 1, which corresponds to an odd coherent state, a coherent state and an even coherent state respectively. As we know, because the interference term in (8) have a rapid decay to a *SM* when we include dissipation, so we want to see how different would be the behaviour of the system if the input states are statistical mixture of the states $|\,\alpha\rangle$ and $|\,-\alpha\rangle$, i.e.,

$$\hat{\rho}(0) = \frac{1}{2}[|\,\alpha\rangle\langle\alpha\,| + |\,-\alpha\rangle\langle-\alpha\,|]\otimes|\,e\rangle\langle e\,|, \tag{9}$$

with

$$|\,\alpha\rangle = \sum_{n=0}^{\infty} q_n\,|\,n\rangle = \sum_{n=0}^{\infty} e^{-\alpha^2/2}\frac{\alpha^n}{\sqrt{n!}}\,|\,n\rangle. \tag{10}$$

Following essentially the same procedures as in Ref. [79] we get the explicit expression of the exact solution of the Milburn equation (2) for the multi-quanta JC model as follows:

$$\begin{aligned}\hat{\rho}(t) &= \sum_{k=0}^{\infty}\frac{1}{k!}\left(\frac{\tau}{\gamma}\right)^k \hat{H}^k\hat{\rho}_2(t)\hat{H}^k \\ &= \sum_{k=0}^{\infty}\frac{1}{k!}\left(\frac{\tau}{\gamma}\right)^k\Big[\hat{M}_{11}^{(k)}(t)\,|\,e\rangle\langle e\,| + \hat{M}_{12}^{(k)}(t)\,|\,e\rangle\langle g\,| \\ &\quad + \hat{M}_{21}^{(k)}(t)\,|\,g\rangle\langle e\,| + \hat{M}_{22}^{(k)}(t)\,|\,g\rangle\langle g\,|\Big],\end{aligned} \tag{11}$$

where the matrices $\hat{M}_{ij}^{(k)}(t)$, $(i, j = 1, 2)$ for the initial condition (9) are given by:

$$\begin{aligned}\hat{M}_{11}^{(k)}(t) &= \hat{A}[\hat{\Psi}_{11}^{+}(t) + \hat{\Psi}_{11}^{-}(t)]\hat{A} \\ &\quad + \hat{A}[\hat{\Psi}_{12}^{+}(t) + \hat{\Psi}_{12}^{-}(t)]\hat{C} + \hat{B}[\hat{\Psi}_{21}^{+}(t) + \hat{\Psi}_{21}^{-}(t)]\hat{A} \\ &\quad + \hat{B}[\hat{\Psi}_{22}^{+}(t) + \hat{\Psi}_{22}^{-}(t)]\hat{C},\end{aligned} \tag{12}$$

$$\hat{M}_{22}^{(k)}(t) = \hat{C}[\hat{\Psi}_{11}^{+}(t) + \hat{\Psi}_{11}^{-}(t)]\hat{B} + \hat{C}[\hat{\Psi}_{12}^{+}(t) + \hat{\Psi}_{12}^{-}(t)]\hat{D} + \hat{D}[\hat{\Psi}_{21}^{+}(t) + \hat{\Psi}_{21}^{-}(t)]\hat{B} + \hat{D}[\hat{\Psi}_{22}^{+}(t) + \hat{\Psi}_{22}^{-}(t)]\hat{D}, \tag{13}$$

and

$$\hat{M}_{21}^{(k)}(t) = [\hat{M}_{12}^{(k)}(t)]^{\dagger} = \hat{C}[\hat{\Psi}_{11}^{+}(t) + \hat{\Psi}_{11}^{-}(t)]\hat{A} + \hat{C}[\hat{\Psi}_{12}^{+}(t) + \hat{\Psi}_{12}^{-}(t)]\hat{C} + \hat{D}[\hat{\Psi}_{21}^{+}(t) + \hat{\Psi}_{21}^{-}(t)]\hat{A} + \hat{D}[\hat{\Psi}_{22}^{+}(t) + \hat{\Psi}_{22}^{-}(t)]\hat{C}, \tag{14}$$

where we have used the following symbol

$$\hat{\Psi}_{ij}^{\pm}(t) = \mid \hat{\Psi}_{i}^{\pm}(t)\rangle\langle\hat{\Psi}_{j}^{\pm}(t) \mid, \quad (i, j = 1, 2) \tag{15}$$

with

$$\hat{A} = \left[\hat{f}^{(k)}(n+m) + \left(\frac{\Delta}{2\lambda}\right)\frac{\hat{g}^{(k)}(n+m)}{\hat{\mu}(n+m)}\right],$$
$$\hat{B} = \hat{R}\frac{\hat{g}^{(k)}(n)}{\hat{\mu}(n)}, \quad \hat{C} = \frac{\hat{g}^{(k)}(n)}{\hat{\mu}(n)}\hat{R}^{\dagger}, \quad \text{and}$$
$$\hat{D} = \left[\hat{f}^{(k)}(n) - \left(\frac{\Delta}{2\lambda}\right)\frac{\hat{g}^{(k)}(n)}{\hat{\mu}(n)}\right], \tag{16}$$

$$\mid \hat{\Psi}_{1}^{\pm}(t)\rangle = \frac{1}{\sqrt{2}}\left[\hat{R}(n+m,t) - \frac{\Delta}{2\lambda}\frac{\hat{V}(n+m,t)}{\hat{\mu}(n+m)}\right]\mid \hat{\psi}^{\pm}(t)\rangle, \tag{17}$$

$$\mid \hat{\Psi}_{2}^{\pm}(t)\rangle = -\frac{1}{\sqrt{2}}\hat{a}^{\dagger m}\left[\frac{\hat{V}(n+m,t)}{\hat{\mu}(n+m)}\right]\mid \hat{\psi}^{\pm}(t)\rangle, \tag{18}$$

where $\mid \hat{\psi}^{\pm}(t)\rangle$ is given by:

$$\mid \hat{\psi}^{\pm}(t)\rangle = \exp\left[-\frac{t}{2\gamma}[\hat{\xi}^{2}(n+m) + \lambda^{2}\hat{\mu}^{2}(n+m)]\right] \times \exp[-i\hat{\zeta}(n+m)t] \mid \pm\alpha\rangle \tag{19}$$

while for the initial condition (8) the matrices $\hat{M}_{ij}^{(k)}(t)$, $(i, j = 1, 2)$ are given by:

$$\hat{M}_{11}^{(k)}(t) = \hat{A}\hat{\Psi}_{11}(t)\hat{A} + \hat{A}\hat{\Psi}_{12}(t)\hat{C} + \hat{B}\hat{\Psi}_{21}(t)\hat{A} + \hat{B}\hat{\Psi}_{22}(t)\hat{C}, \tag{20}$$

$$\hat{M}_{22}^{(k)}(t) = \hat{C}\hat{\Psi}_{11}(t)\hat{B} + \hat{C}\hat{\Psi}_{12}(t)\hat{D} + \hat{D}\hat{\Psi}_{21}(t)\hat{B} + \hat{D}\hat{\Psi}_{22}(t)\hat{D}, \tag{21}$$

and

$$\hat{M}_{21}^{(k)}(t) = [\hat{M}_{12}^{(k)}(t)]^{\dagger} = \hat{C}\hat{\Psi}_{11}(t)\hat{A} + \hat{C}\hat{\Psi}_{12}(t)\hat{C} + \hat{D}\hat{\Psi}_{21}(t)\hat{A} + \hat{D}\hat{\Psi}_{22}(t)\hat{C}, \tag{22}$$

where

$$\hat{\Psi}_{ij}(t) = \mid \hat{\Psi}_i(t) > < \hat{\Psi}_j(t) \mid, \quad (i,j=1,2) \tag{23}$$

with

$$\begin{aligned} \mid \hat{\Psi}_1(t)\rangle = \frac{1}{\sqrt{L}}\left[\hat{R}(n+m,t) - \frac{\Delta}{2\lambda}\frac{\hat{V}(n+m,t)}{\hat{\mu}(n+m)}\right] \\ \times [\mid \hat{\psi}^+(t)\rangle + r \mid \hat{\psi}^-(t)\rangle], \end{aligned} \tag{24}$$

$$\mid \hat{\Psi}_2(t)\rangle = -\frac{1}{\sqrt{L}}\hat{a}^{\dagger m}\left[\frac{\hat{V}(n+m,t)}{\hat{\mu}(n+m)}\right][\mid \hat{\psi}^+(t)\rangle + r \mid \hat{\psi}^-(t)\rangle], \tag{25}$$

where $\mid \hat{\psi}^{\pm}(t)\rangle$ is given by (19) and

$$\hat{R}(n,t) = \cos\lambda t\hat{\mu}(n)\cosh\left[\frac{\lambda t}{\gamma}\hat{\zeta}(n)\hat{\mu}(n)\right] + i\sin\lambda t\hat{\mu}(n)\sinh\left[\frac{\lambda t}{\gamma}\hat{\zeta}(n)\hat{\mu}(n)\right] \tag{26}$$

$$\hat{V}(n,t) = \cos\lambda t\hat{\mu}(n)\sinh\left[\frac{\lambda t}{\gamma}\hat{\zeta}(n)\hat{\mu}(n)\right] + i\sin\lambda t\hat{\mu}(n)\cosh\left[\frac{\lambda t}{\gamma}\hat{\zeta}(n)\hat{F}(n)\right], \tag{27}$$

and

$$\begin{aligned} \hat{f}^{(k)}(n) &= \frac{1}{2}[\hat{\Phi}^k(n,+) + \hat{\Phi}^k(n,-)], \\ \hat{g}^{(k)}(n) &= \frac{1}{2}[\hat{\Phi}^k(n,+) - \hat{\Phi}^k(n,-)], \end{aligned} \tag{28}$$

where the operators $\hat{\Phi}(n,+)$ and $\hat{\Phi}(n,-)$ are defined by

$$\hat{\Phi}(n,\pm) = \hat{\zeta}(n) \pm \lambda\hat{F}(n), \tag{29}$$

$$\begin{aligned} \hat{\mu}^2(n) &= \left(\frac{\Delta}{2\lambda}\right)^2 + \hat{\nu}^2(n), \quad \hat{\nu}^2(n) = \frac{n!}{(n-m)!}, \\ \hat{\zeta}(n) &= \omega\left(\hat{n} - \frac{m}{2}\right). \end{aligned} \tag{30}$$

We can obtain the reduced density operator for the particle by taking the trace over the states of the field. Thus the reduced density particle operator becomes

$$\hat{\rho}_a(t) = Tr_f\hat{\rho}(t) = \begin{bmatrix} C_{11}(t) & C_{12}(t) \\ C_{21}(t) & C_{22}(t) \end{bmatrix}, \tag{31}$$

where

$$C_{ij}(t) = \sum_{k,n=0}^{\infty}\frac{1}{k!}\left(\frac{\tau}{\gamma}\right)^k \langle n \mid \hat{M}_{ij}^{(k)}(t) \mid n\rangle \tag{32}$$

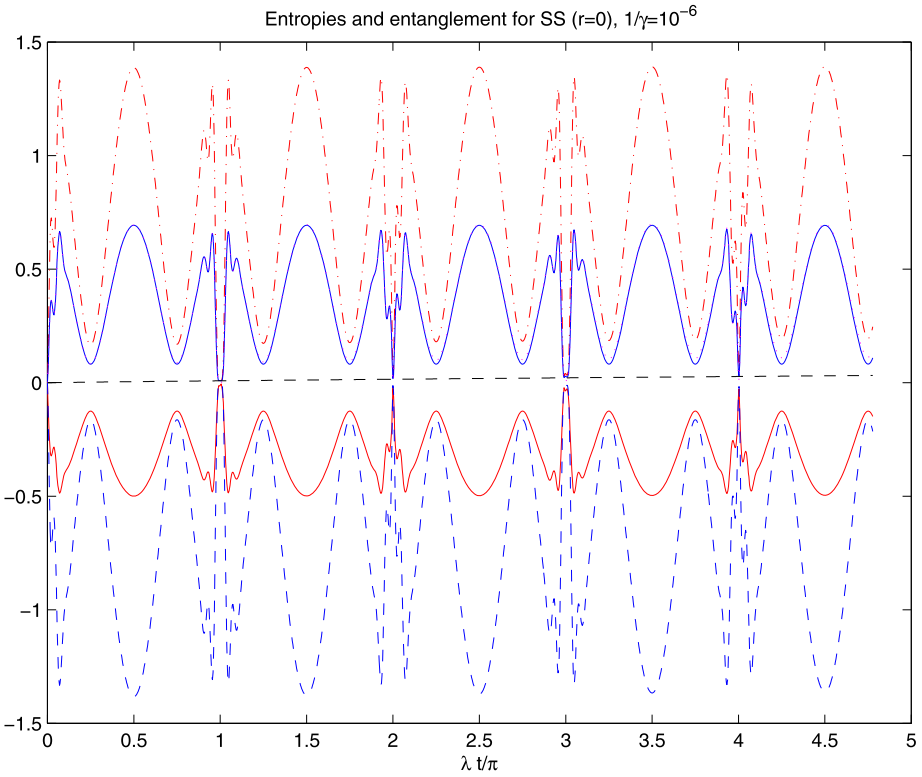

Fig. 1 Partial entropy $S_a(t)$ for the atom (*upper solid line*), $S_f(t)$ the field (*dotted line*) as well as the total entropy $S(t)$ (*dashed line*) and $S_a(t) + S_f(t)$ (*dot-dashed line*) as a function of the scaled time λt of the particle initially prepared in the excited state and the field initially prepared in a superposition state *SS* ($r = 0$ (coherent state)) $|\alpha\rangle$ ($\bar{n} = 16$), for small decoherence $1/\gamma = 10^{-6}$. The *lower solid line* shows the sum of the negative eigenvalues $E_N(t)$ of the partially transposed density matrix ρ^{T_A} in comparison to the entropy difference $E_D(t)$ (*lower dashed line*)

while the reduced density operator for the field is given by

$$\hat{\rho}_f(t) = Tr_a\hat{\rho}(t) = \sum_{k=0}^{\infty} \frac{1}{k!}\left(\frac{\tau}{\gamma}\right)^k \left[\hat{M}_{11}^{(k)}(t) + \hat{M}_{22}^{(k)}(t)\right]. \tag{33}$$

Employing the density operator and the reduced density operators for the particle or the field are given by (11) and (31), (33), we investigate the properties of the evolution of the degree of entanglement.

3 Degree of Entanglement

Despite the fact that the possibility of quantum entanglement was acknowledged almost as soon as quantum theory was discovered, it is only in the last few years that consideration has been given to finding mathematical methods to quantify entanglement. The first point to note is that no measure of entanglement can be linear in the system state. This follows directly

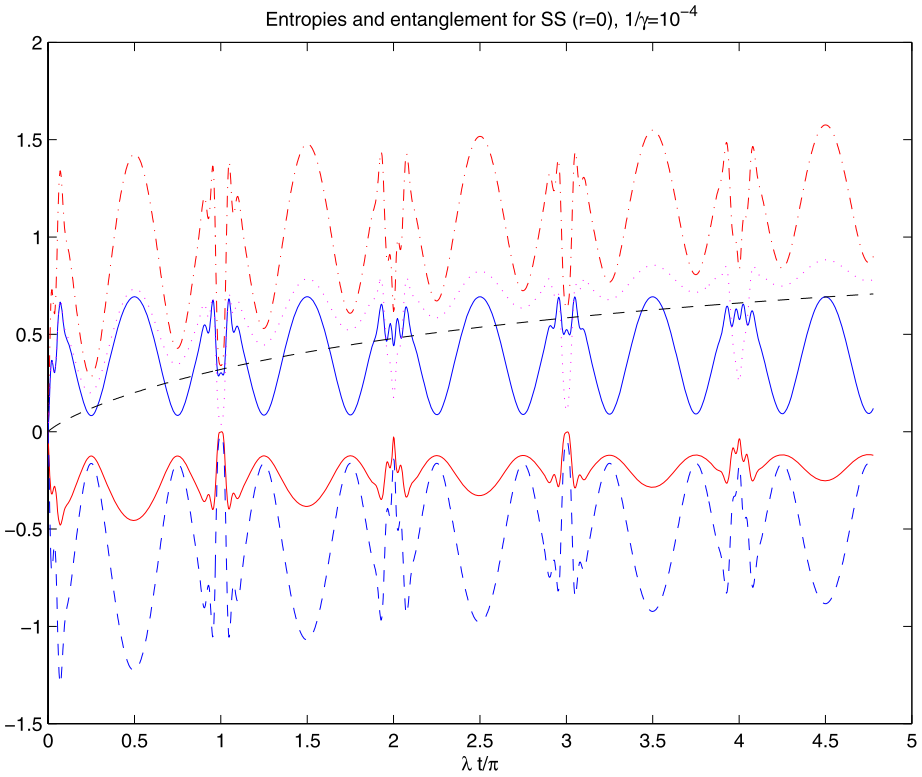

Fig. 2 Same as Fig. 1 for the decoherence $1/\gamma = 10^{-4}$

from the fact that the entanglement is invariant under local unitary transformation. In the case of pure quantum state for two subsystem, a number of physically intuitive measures of entanglement have been known for some time. However, for general mixed states of an arbitrary number of subsystems, entanglement measures are still under development.

In this article, we use the field entropy as a measure of the degree of entanglement between the field and the particle of the system under consideration.

The entropy S of the quantum-mechanical system can be defined as follows:

$$S = -Tr\{\hat{\rho} ln \hat{\rho}\}, \tag{34}$$

where we have set the Boltzmann constant K equal to unity. If $\hat{\rho}$ describes a pure state, then $S = 0$, and if $\hat{\rho}$ describes a mixed state, then $S \neq 0$. Entropies of the atomic and field sub-systems are defined by the corresponding reduced density operators:

$$S_{a(f)} = -Tr_{a(f)}\{\hat{\rho}_{a(f)} ln \rho_{a(f)}\}. \tag{35}$$

For the entropy of a general two-component system one has the Araki-Lieb theorem [80]: $\mid S_a - S_f \mid \leq S \leq S_a + S_f$. One immediate consequence of this inequality is that if the total system is in a pure state then its total entropy vanishes and the component systems have equal entropies [1–3, 5]. If these are nonzero, it clearly proves entanglement in this case, as for any product density operator the total entropy is less than the sum of the subsystem

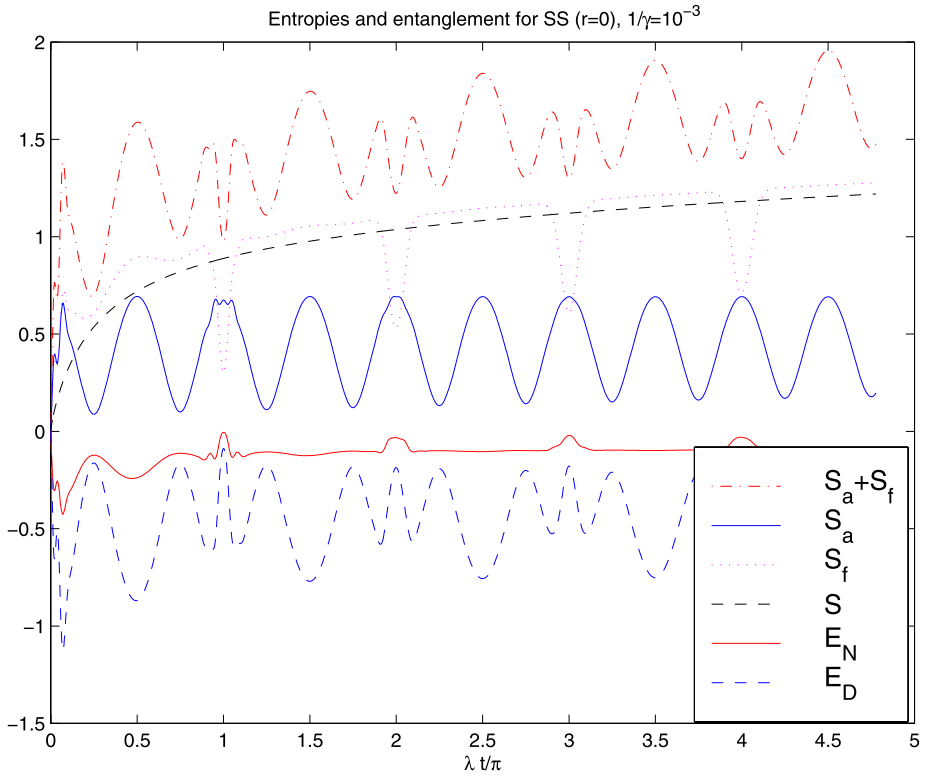

Fig. 3 Same as Fig. 1 for the decoherence $1/\gamma = 10^{-3}$

entropies. For a general state one has entanglement, if the subsystem entropies have a sum bigger than the total entropy.

We shall consider the entropy difference E_D defined by

$$E_D = \frac{1}{4}(S - S_a - S_f). \tag{36}$$

Negative values of this quantity means a degree of entanglement. We will compare this difference with the sum of negative eigenvalues of the partially transposed density matrix denoted by E_N. This latter quantity has been recently proposed as a quantitative entanglement measure [81]. This partial transpose takes the form of a direct sum, such that the spectrum of the transposed matrix ρ^{T_A} of the density matrix ρ can be evaluated from the spectrum of each block. The negative eigenvalues of this spectrum are then summed to give the value E_N. We make a comparison between these two quantities, however the question of quantifying the degree of entanglement for general mixed states is still under discussion [82–84].

4 Numerical Results and Discussion

The numerical results are presented in Figs. 1–9, we display the entropy for the atom S_a, field entropy S_f as well as the total entropy S, sum of the partial entropies, entropy difference

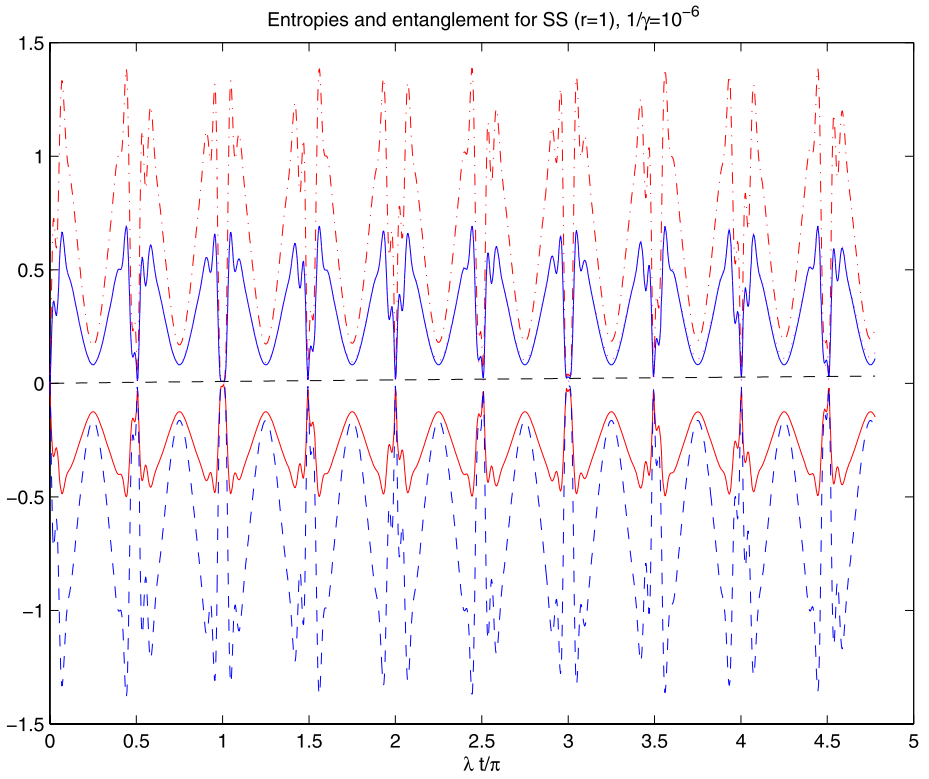

Fig. 4 Partial entropy $S_a(t)$ for the atom (*upper solid line*), $S_f(t)$ the field (*dotted line*) as well as the total entropy $S(t)$ (*dashed line*) and $S_a(t) + S_f(t)$ (*dot-dashed line*) as a function of the scaled time λt of the particle initially prepared in the excited state and the field initially prepared in a superposition state *SS* ($r = 1$ (even coherent state)) $|\alpha\rangle$ ($\bar{n} = 16$), for small decoherence $1/\gamma = 10^{-6}$. The *lower solid line* shows the sum of the negative eigenvalues $E_N(t)$ of the partially transposed density matrix ρ^{T_A} in comparison to the entropy difference $E_D(t)$ (*lower dashed line*)

E_D and sum of the negative eigenvalues of the partially transposed density matrix E_N for various values of the decoherence parameter $\frac{1}{\gamma}$, with fixed initial mean number of quanta $\bar{n} = 16$ as functions of the scaled time λt for the exact resonance case i.e., the detuning parameter $(\frac{\Delta}{2\lambda}) = 0$.

In Figs. 1–6, we plot the entropy for the atom S_a, field entropy S_f as well as the total entropy S, sum of the partial entropies, entropy difference E_D and sum of the negative eigenvalues of the partially transposed density matrix E_N for three values of the parameter $\frac{1}{\gamma}$ for the field initially in a superposition state (*SS*), while for the statistical mixture state (*SM*) are presented in Figs. 7–9.

Now we investigate the influence of the intrinsic decoherence on the evolution of the field-, atom- and total entropy numerically. We display the evolution of the entropies for the atom initially prepared in the excited state and the field in a superposition state (*SS*) ($r = 1$) coherent state as functions of the scaled time ($0 \leq \lambda t \leq 15$) for the two-quanta process ($m = 2$) for various values of the decoherence parameter γ. Here we assume a coherent field state with initial mean number of quanta $\bar{n} = 16$ initially to provide for a strong coupling.

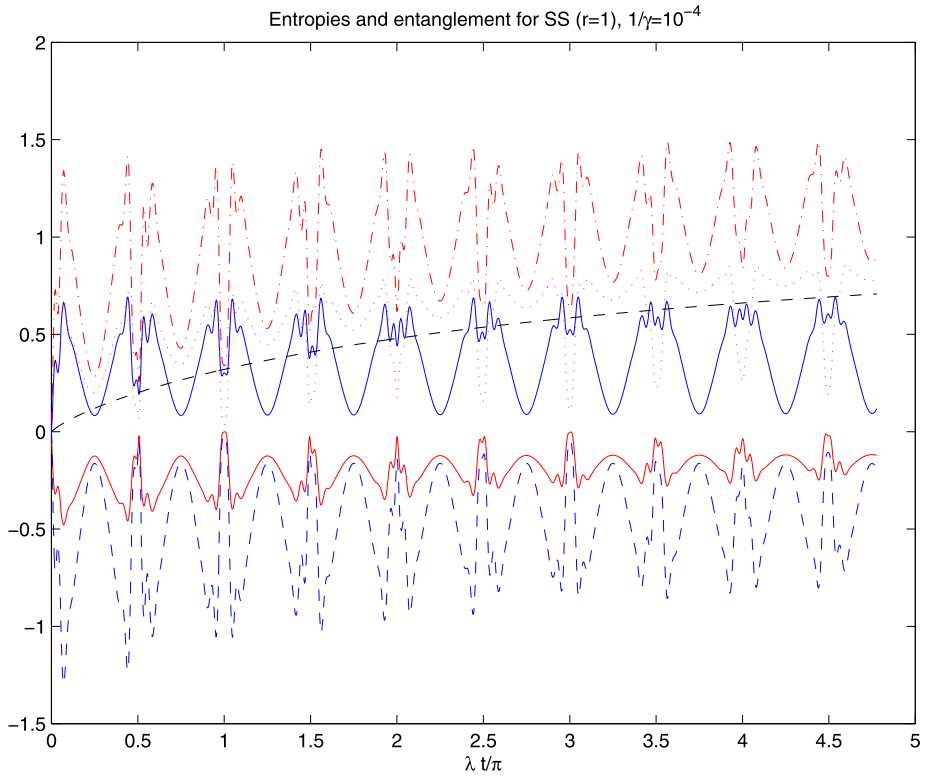

Fig. 5 Same as Fig. 4 for the decoherence $1/\gamma = 10^{-4}$

The sensitivity becomes even more clearly visible, when we show the total entropy of the system S and compare it to the sum of partial entropies $S_a + S_f$, the sum of negative eigenvalues E_N of ρ^{T_A}, and entropy difference E_D.

In Fig. 1 we show the time evolution of the partial atomic and field entropies (S_a, S_f) and the total entropy S for very weak decoherence $\gamma = 10^6$. The atomic inversion show regularity in this case and periodicity of π for the revivals [5, 8]. As entropy measures we plot the sum of the negative eigenvalues E_N of the partially transposed density matrix ρ^{T_A} and the entropy difference E_D on the same figure. Note that both S_f and S_a are larger than S (which is zero) at any time for the time interval considered. However for very long time periods $(\lambda t > 10^3)$ the features appearing in the case of $\gamma \sim 10^3$ in Fig. 3 become pronounced here as well.

From this figure (Fig. 1), as one could expect when $(\gamma \to \infty)$, the field and the atom entropy evolve with a period $\frac{\pi}{\lambda}$ (see Fig. 1 upper solid line and dotted line which are the same) and reaches zero at times $\lambda t = n\pi$ $(n = 0, 1, 2, 3\ldots)$. In accordance with the picture of the collapses and revivals of the two-photon JC model investigated by many authors in the literature. Here the field is completely disentangled from the particle. For other times $\lambda t = (n + \frac{1}{2})\pi$, it evolves to the maximum value, and the field is strongly entangled with the particle. Between these extreme points the entropies S_f and S_a reach minimum values for $\gamma = 10^6$ and both of them are equal in this case. However as γ decreases we find that the two quantities start to depart. The entropy for the atom changes its characters and differs greatly

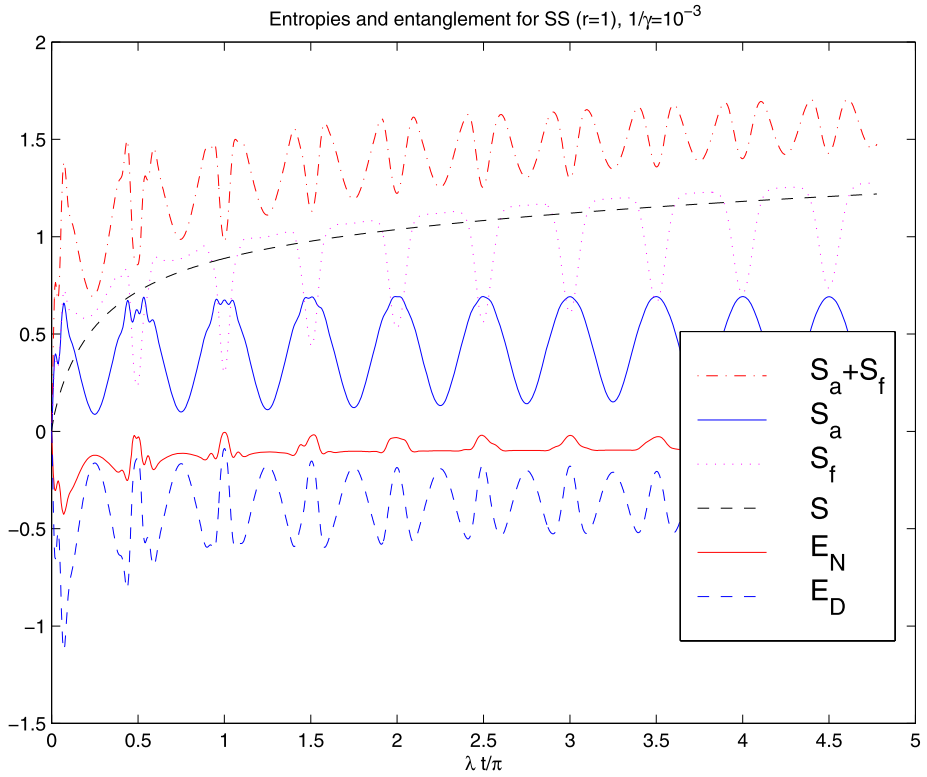

Fig. 6 Same as Fig. 4 for the decoherence $1/\gamma = 10^{-3}$

from the field entropy. While the field still reaches its minima at $\lambda t = n\pi$ the atomic entropy becomes maxima at these points (see Fig. 3 upper solid line and dotted line for $\gamma = 10^3$). On the other hand the entropy for the atom (upper solid line) reaches its minima at almost $\lambda t = (n + \frac{1}{4})\pi$ and $(n + \frac{3}{4})\pi$, the field entropy (dotted line) develops an almost constant at maximum values along the interval $n\pi < \lambda t < (n+1)\pi$ between its minima. Also we show in these figures how the total entropy S increases as time develops when the parameter γ is decreased, and hence decoherence is more effective.

Figures 2 and 3 are the same as in Fig. 1, but for the decoherence parameter $\gamma = 10^4$ and 10^3, respectively. It is to be remarked that S_f is always larger than S of the total system except at $\lambda t = n\pi$, S_a on the other hand may be less than S, ($S_a < S$ for $\lambda t > \pi/2$ when $\gamma = 10^3$). It is to be observed that as time develops the negativity of both E_D and E_N becomes smaller. This means that the degree of entanglement becomes weaker. These figures show that with the decreasing of the parameter γ, we observe rapid deterioration of the revivals of the field and atom entropy. This shows a very fast decay of quantum entanglement due to decoherence in the multi-quanta JC model with a rate more rapid than in the standard JC model discussed earlier [79]. As it has been discussed above, the decoherence amounts statistical mixtures of states result and consequently the entropies of the subsystems start to differ and the total entropy increases.

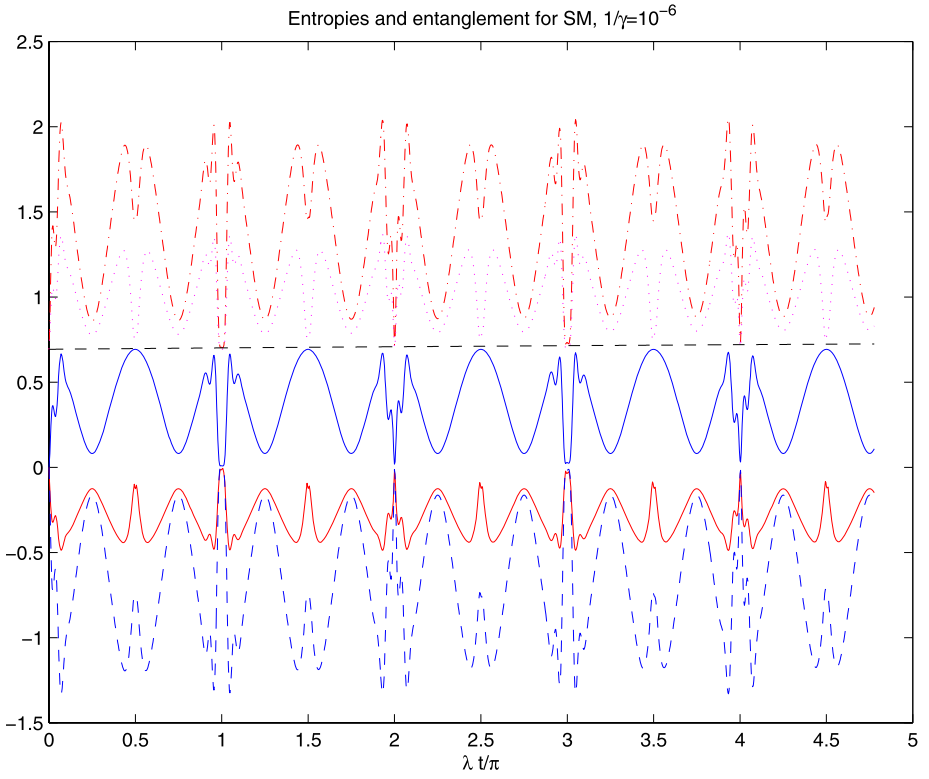

Fig. 7 Partial entropy $S_a(t)$ for the atom (*upper solid line*), $S_f(t)$ the field (*dotted line*) as well as the total entropy $S(t)$ (*dashed line*) and $S_a(t) + S_f(t)$ (*dot-dashed line*) as a function of the scaled time λt of the particle initially prepared in the excited state and the field initially prepared in a *SM* of coherent states $|\alpha\rangle$ and $|-\alpha\rangle$ ($\bar{n} = 16$), for small decoherence $1/\gamma = 10^{-6}$. The *lower solid line* shows the sum of the negative eigenvalues $E_N(t)$ of the partially transposed density matrix ρ^{T_A} in comparison to the entropy difference $E_D(t)$ (*lower dashed line*)

In Figs. 1–3, we show the time evolution of the entropy difference E_D and sum of the negative eigenvalues of the partially transposed density matrix E_N. As we see from these figures, we get strong entanglement, which is well reflected as a very good entropy measure.

Here again we note that E_N and E_D show the same characteristics for the maxima and minima for large γ. But as γ decreases to 10^3 it is observed that E_D shows more fluctuations than E_N. However the maxima occur at $\lambda t = n\pi$ in both figures and as γ decreases neither E_N nor E_D reaches the value zero for any time $t > 0$ which means that disentanglement does not occur at any time later.

In Figs. 4–6, we display the time evolution of the partial atomic and field entropies (S_a, S_f) as well as the total entropy S, sum of the partial entropies, entropy difference E_D and sum of the negative eigenvalues of the partially transposed density matrix E_N for three values of the parameter $\frac{1}{\gamma}$ for the field initially in a superposition state (SS) $(r = 1)$ (even coherent state).

As we see from Fig. 4 for very weak decoherence $\gamma = 10^6$, both the field S_f and the atom entropy S_a are the same and larger than S (which is zero) (see Fig. 4 upper solid and dotted curve), and it evolves with a period $\frac{1}{2}\frac{\pi}{\lambda}$ and reaches zero at times $\lambda t = \frac{n\pi}{2}$ $(n = 0, 1, 2, 3\ldots)$

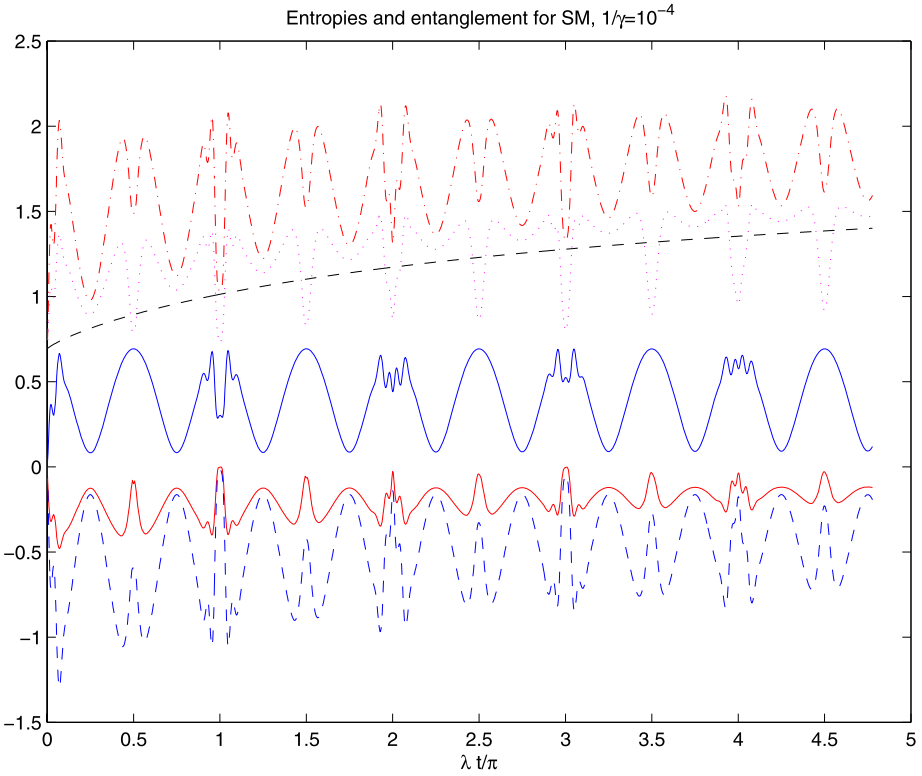

Fig. 8 Same as Fig. 7 for the decoherence $1/\gamma = 10^{-4}$

i.e. at half of the revival time for the *SM*. Here the field is completely disentangled from the particle. For other times $\lambda t = (2n+1)\frac{\pi}{4}$, it evolves to the minimum value, and the field is weakly entangled with the particle.

This effect is due to the interference between the two coherent states in the superposition, and can be understood looking at the photon number distribution of the initial fields. Hence this signal gives a clear measure of the remaining degree of coherence between the two components of the cat state, while the signals present in both cases are due to intrinsic revivals of each component individually.

Figures 5 and 6 are the same as in Fig. 4, but for the decoherence parameter $\gamma = 10^4$ and 10^3, respectively. It is to be remarked that the total entropy S increases and the field entropy S_f is always larger than S of the total system except $\lambda t = \frac{n\pi}{2}$, S_a on the other hand may be less than S, ($S_a < S$ for $\lambda t > \pi/2$ when $\gamma = 10^3$). It is to be observed that as time develops the negativity of both E_D and E_N becomes smaller. This means that the degree of entanglement becomes weaker.

In Fig. 7, we plot the entropy for the atom S_a, field entropy S_f as well as the total entropy S, sum of the partial entropies, entropy difference E_D and sum of the negative eigenvalues of the partially transposed density matrix E_N for very weak decoherence $\gamma = 10^6$ when the field initially in statistical mixture state (*SM*).

As we see from this figure the field entropy S_f is not equal the atomic entropy S_a and S_f is grater than the total entropy S (which is not equal 0 in this case (see Fig. 7 upper solid,

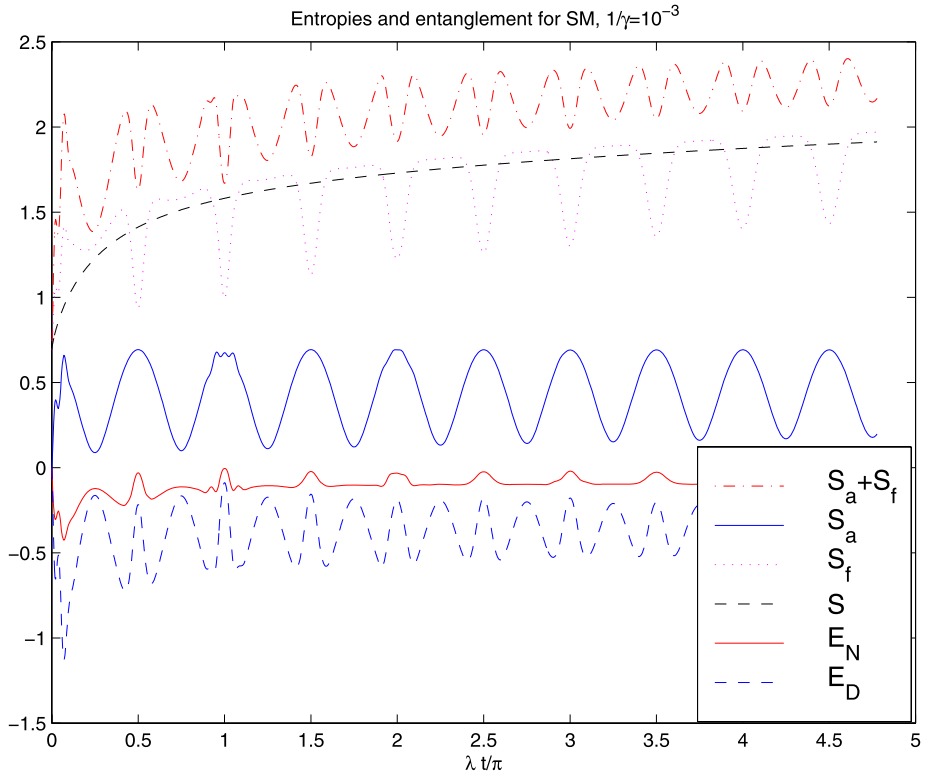

Fig. 9 Same as Fig. 7 for the decoherence $1/\gamma = 10^{-3}$

dotted and dashed curve), while the atomic entropy is less than the total entropy S ($S_a < S$ for the time interval considered) and it evolve with a period $\frac{\pi}{\lambda}$ and reaches zero at times $\lambda t = n\pi$ $(n = 0, 1, 2, 3\ldots)$ i.e. at the revival time for the *SM*. As we noted in the statistical mixture state, ($S_f \neq S_a$), the entropy for the atom reaches maximum values at half of the revival time, while S_f evolves to its minimum vales. For comparison purposes, we have chosen to set different values of the decoherence parameter γ and other parameters which are the same as in Fig. 7. The outcome is presented in Fig. 8 (where $\gamma = 10^4$) and Fig. 9 (where $\gamma = 10^3$).

These figures show that with the decreasing of the parameter γ, we observe rapid deterioration of the revivals of the field and atom entropy. This shows a very fast decay of quantum entanglement due to the very specific time evolution described by the Milburn equation (2), i.e., due to the intrinsic decoherence.

The evolution of the entropy for the atom S_a, field entropy S_f as well as the total entropy S, sum of the partial entropies, entropy difference E_D and sum of the negative eigenvalues of the partially transposed density matrix E_N for either superposition states (*SS*) or a statistical mixture (*SM*) of coherent states for $m > 2$ (for example $m = 3, 4$) could be considered and the effects of the multi-quanta on the entropies and entanglement could be discussed. From numerical results (not demonstrated here), we note that with the increase of the parameter m, i.e. with increase of the number of quanta, we observe a rapid increase of the degree of the entanglement for the same values of the parameter γ. It is also

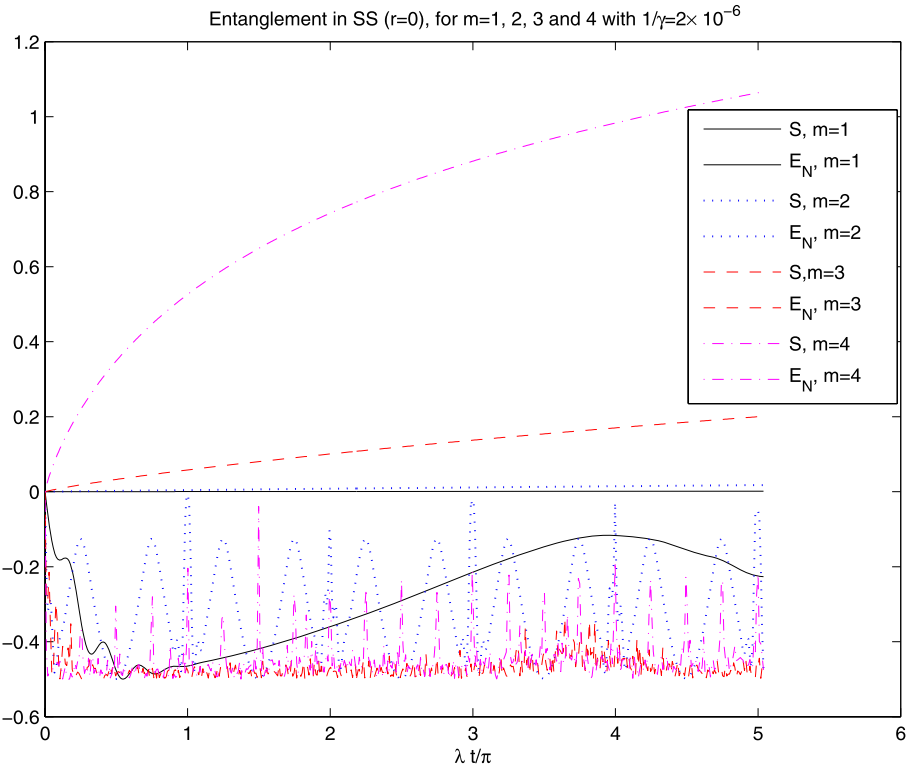

Fig. 10 Time evaluation of the total entropy $S(t)$ (*upper solid*, *dotted*, *dashed* and *dot-dashed curves* for $m = 1, 2, 3$, and 4 respectively) as well as the negativity $E_N(t)$ (*lower curves* (*solid*, *dotted*, *dashed* and *dot-dashed curves* for $m = 1, 2, 3$, and 4 respectively)) as a function of the scaled time λt of the particle initially prepared in the excited state and the field initially prepared in a superposition state *SS* ($r = 0$ (coherent state)) $|\alpha\rangle$ ($\bar{n} = 16$), for small decoherence $2/\gamma = 10^{-6}$

to be remarked that the entropies and the entanglement depend on the number of the quanta transition m.

To show this we investigate the relationship between the entanglement and both of gamma and multi-quanta number m. Also the entanglement for the multi-quanta due to the decoherence can be considered and the effects of the number of quanta on the entanglement for either initial pure state (*SS*) or initial mixed state (mixture state (*SM*)) could be discussed.

In Figs. 10–12, as measure of entanglement with the number of quanta m and decoherence parameter γ, we plot the total entropy S as well as the sum of the negative eigenvalues of the partially transposed density matrix E_N for some numbers of multiplicity m (namely $m = 1, 2, 3$ and 4) for the three values of the decoherence parameter γ in the superposition states (*SS*, $r = 0$). These figures show that by increasing the number of quanta m the entanglement increases monotonically (see Figs. 10–12). So, we get strong entanglement by increasing the number of quanta transitions m.

It is also to be remarked that the entanglement is not depending on the number of the quant transition m only but also depending on the decoherence parameter γ.

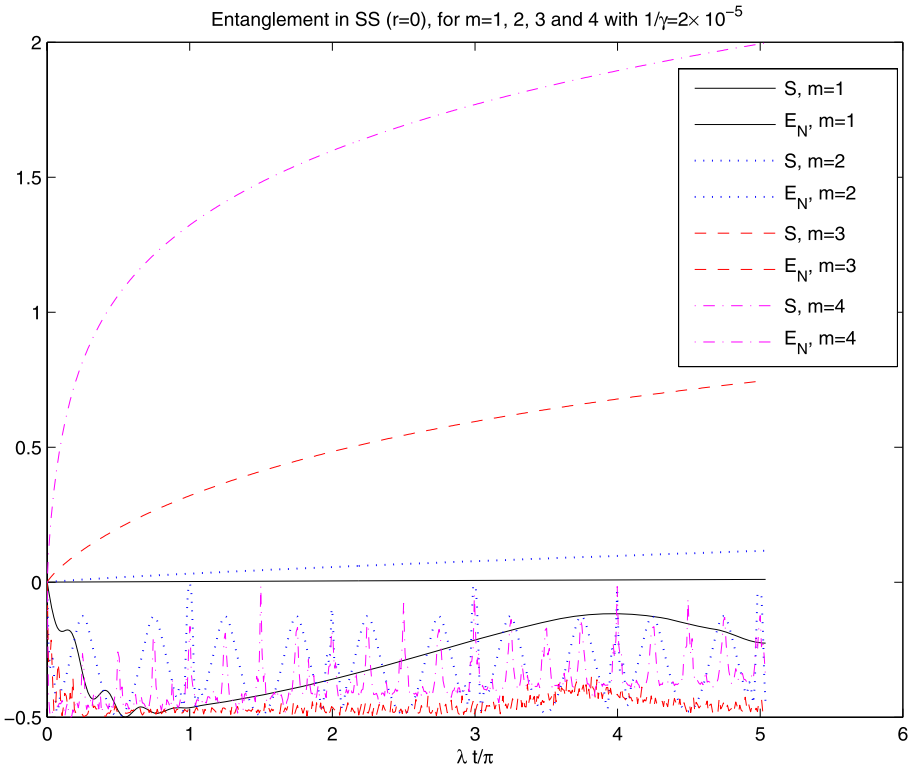

Fig. 11 Same as Fig. 10 for the decoherence $2/\gamma = 10^{-5}$

From numerical results for the superposition states (SS, $r = 1$ (even coherent state)) and mixture state (SM) (not show here), we note that the two cases are more affected than the superposition states (SS, $r = 0$), but it is more effective on the mixture state (SM).

Thus we conclude that both the number of quanta m and initial field (SS or SM) affect the entanglement as well as the decoherence parameter γ. Furthermore the initial mixed state (statistical mixture state (SM)) has much more effect than the initial pure state (SS).

5 Summary

In this paper, using an established entanglement measure based on the negativity of the eigenvalues of the partially transposed density matrix we have studied the entropy growth and degradation of entanglement due to intrinsic decoherence for the initial mixed state in the multi-quanta JC model. The work here extends previous studies in this context. We find an exact solution of the Milburn equation for the two-level particle (atom or trapped ion) and calculate the partial entropy of the particle and field subsystem as well as total entropy. Then it is used to study how intrinsic decoherence leads to growing entropy and a strong degradation of the maximal generated entanglement in the multi-quanta JC model. We find that the relative size of the partial system entropies and the total entropy provides for qualitatively correct estimate of entanglement, but shows only limited quantitative agreement with an alternative entanglement measure using the maximum negative eigenvalue of the partially

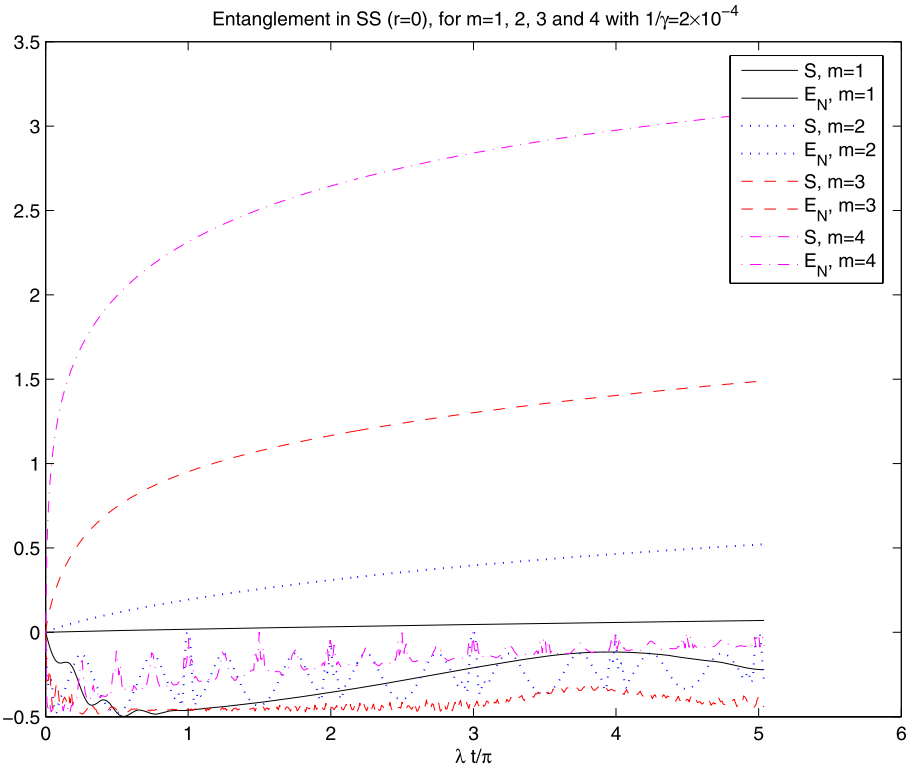

Fig. 12 Same as Fig. 10 for the decoherence $2/\gamma = 10^{-4}$

transposed density matrix. Surprisingly the agreement of the two measures is different for energy loss and decoherence. Also, by decreasing the parameter γ in either *SS* (even coherent state) or *SM* the particle and the field are strongly entanglement. Furthermore both the number of quanta m and initial field (*SS* or *SM*) affect the entanglement as well as the decoherence parameter γ and the initial mixed state has much more effect than the initial pure state.

Acknowledgement The author wish to record his thanks to the referees for their valuable comments that resulted in improvements of the article in many aspects.

References

1. Phoenix, S.J.D., Knight, P.L.: Ann. Phys. **186**, 381 (1988)
2. Phoenix, S.J.D., Knight, P.L.: Phys. Rev. A **44**, 6023 (1991)
3. Phoenix, S.J.D., Knight, P.L.: Phys. Rev. Lett. **66**, 2833 (1991)
4. Buzek, V., Moya-Cessa, H., Knight, P.L., Phoenix, S.J.D.: Phys. Rev. A **45**, 8190 (1992)
5. Phoenix, S.J.D., Knight, P.L.: J. Opt. Soc. Am. B **7**, 116 (1990)
6. Knight, P.L., Shore, B.W.: Phys. Rev. A **48**, 642 (1993)
7. Buzek, V., Hladky, B.: J. Mod. Opt. **40**, 1309 (1993)
8. Fang, M.F., Zhou, G.H.: Phys. Lett. A **184**, 397 (1994)
9. Fang, M.F.: J. Mod. Opt. **41**, 1319 (1994)
10. Fang, M.F.: Acta Phys. Sin. **43**, 1776 (1994)

11. Fang, M.F., Zhou, P.: Acta Phys. Sin. **43**, 570 (1994)
12. Fang, M.F., Zhou, P.: Acta Opt. Sin. **13**, 799 (1993)
13. Fang, M.F., Zhou, P.: Acta Opt. Sin. **14**, 475 (1994)
14. Cirac, J.I., Zoller, P.: Phys. Rev. Lett. **74**, 4091 (1995)
15. Monroe, C., Meekhof, D.M., King, B.E., Itano, W.M., Wineland, D.J.: Phys. Rev. Lett. **75**, 4714 (1995)
16. Roos, C., Zeiger, T., Rohde, H., Nagerl, H.C., Eschner, J., Leibfried, D., Schmidt-Kaler, F., Blatt, R.: Phys. Rev. Lett. **83**, 4713 (1999)
17. Monroe, C., Meekhof, D.M., King, B.E., Jefferts, S.R., Itano, W.M., Wineland, D.J., Gould, P.: Phys. Rev. Lett. **75**, 4011 (1995)
18. Meekhof, D.M., Monroe, C., King, B.E., Itano, W.M., Wineland, D.J.: Phys. Rev. Lett. **76**, 1796 (1996)
19. Leibfried, D., Meekhof, D.M., King, B.E., Wineland, D.J.: Phys. Rev. Lett. **77**, 4281 (1996)
20. Monroe, C., Meekhof, D.M., King, B.E., Wineland, D.J.: Science **272**, 1131 (1996)
21. Itano, W.M., Monroe, C., Meekhof, D.M., Leibfried, D., King, B.E., Wineland, D.J.: SPIE Proc. Phys. Rev. Lett. **43**, 2995 (1997)
22. King, B.E., Wood, C.S., Myatt, C.J., Turchette, Q.A., Leibfried, D., Itano, W.M., Monroe, C., Wineland, D.J.: Phys. Rev. Lett. **81**, 1525 (1998)
23. Wallentowitz, S., Vogel, W.: Phys. Rev. Lett. **75**, 2932 (1995)
24. de Matos Filho, R.L., Vogel, W.: Phys. Rev. A **50**, R1988 (1994)
25. de Matos Filho, R.L., Vogel, W.: Phys. Rev. Lett. **76**, 4520 (1996)
26. Wallentowitz, S., de Matos Filho, R.L., Vogel, W.: Phys. Rev. A **56**, 1205 (1997)
27. Poyatos, J.F., Cirac, J.I., Zoller, P.: Phys. Rev. Lett. **77**, 4728 (1996)
28. Poyatos, J.F., Walser, R., Cirac, J.I., Zoller, P.: Phys. Rev. A **53**, R1966 (1996)
29. D'Helon, C., Milburn, G.J.: Phys. Rev. A **52**, 4755 (1995)
30. Bardoff, P.J., Leichtle, C., Schrade, G., Schleich, W.P.: Phys. Rev. Lett. **77**, 2198 (1996)
31. Kneer, B., Law, C.K.: Phys. Rev. A **57**, 2096 (1998)
32. Gou, S.-C., Knight, P.L.: Phys. Rev. A **54**, 1682 (1996)
33. Gou, S.-C., Steinbach, J., Knight, P.L.: Phys. Rev. A **54**, R1014 (1996)
34. Gou, S.-C., Steinbach, J., Knight, P.L.: Phys. Rev. A **54**, 4315 (1996)
35. Gou, S.-C., Steinbach, J., Knight, P.L.: Phys. Rev. A **55**, 3719 (1996)
36. Gerry, C.C., Gou, S.-C., Steinbach, J.: Phys. Rev. A **55**, 630 (1997)
37. Steinbach, J., Twamley, J., Knight, P.L.: Phys. Rev. A **56**, 4815 (1997)
38. Bachor, H.A.: A Guide to Experiments in Quantum Optics, chapter 12. Wiley-VCH, Weinheim (1998)
39. Bachor, H.A.: Nuovo Cimento **73B**, 27 (1983) (reprint)
40. Blockley, C.A., Walls, D.F., Risken, H.: Europhys. Lett. **17**, 509 (1992)
41. Blockley, C.A., Walls, D.F.: Phys. Rev. A **47**, 2115 (1993)
42. Cirac, J.I., Blatt, R., Parkins, A.S., Zoller, P.: Phys. Rev. Lett. **70**, 762 (1993)
43. Cirac, J.I., Parkins, A.S., Blatt, R., Zoller, P.: Phys. Rev. Lett. **70**, 556 (1993)
44. Cirac, J.I., Blatt, R., Zoller, P., Phillips, W.D.: Phys. Rev. A **46**, 2668 (1992)
45. Cirac, J.I., Blatt, R., Parkins, A.S., Zoller, P.: Phys. Rev. A **48**, 2169 (1993)
46. Jaynes, E.T., Cummings, F.W.: Proc. IEEE **51**, 89 (1963)
47. Vogel, W., de Matos Filho, R.L.: Phys. Rev. A **52**, 4214 (1995)
48. Buzek, V., Drobny, G., Kim, M.S., Adam, G., Knight, P.L.: Phys. Rev. A **56**, 2352 (1997)
49. Shore, P.W.: Phys. Rev. A **52**, R2493 (1995)
50. Chuang, I.L., Yamamoto, Y.: Phys. Rev. A **55**, 114 (1997)
51. Ghirardi, G.C., Rimini, A., Weber, T.: Phys. Rev. D **34**, 470 (1986)
52. Caves, C.M., Milburn, G.J.: Phys. Rev. D **36**, 5543 (1987)
53. Diosi, L.: Phys. Rev. A **40**, 1165 (1989)
54. Ellis, J., Mohanty, S., Nanopaulos, D.V.: Phys. Lett. B **221**, 113 (1989)
55. Ellis, J., Mohanty, S., Nanopaulos, D.V.: Phys. Lett. **235**, 305 (1990)
56. Ghirardi, G.C., Pearle, P., Rimini, A.: Phys. Rev. A **42**, 78 (1990)
57. Ghirardi, G.C., Grassi, R., Rimini, A.: Phys. Rev. A **42**, 1057 (1990)
58. Milburn, G.J.: Phys. Rev. A **44**, 5401 (1991)
59. Milburn, G.J.: Phys. Rev. A **47**, 2415 (1993)
60. Moya-Cessa, H., Buzek, V., Kim, M.S., Knight, P.L.: Phys. Rev. A **48**, 3900 (1993)
61. Kuang, L.-M., Chen, X.: J. Phys. A **27**, L663 (1994)
62. Chen, X., Kuang, L.-M.: Phys. Lett. A **191**, 18 (1994)
63. Kuang, L.-M., Chen, X., Ge, M.-L.: Phys. Rev. A **52**, 1857 (1995)
64. Obada, A.-S.F., Abdel-Hafez, A.M., Hessian, H.A.: Acta Phys. Slovaca **49**, 381 (1999)
65. Obada, A.-S.F., Abdel-Hafez, A.M., Hessian, H.A.: J. Phys. B **31**, 5085 (1998)
66. Hessian, H.A.: Int. J. Theor. Phys. **41**, 1397 (2002)
67. Omne's, R.: Phys. Rev. A **56**, 3383 (1997)

68. Brune, M., Hagley, E., Dreyer, J., Maitre, X., Maali, A., Wunderlich, C., Raimond, J.M., Haroche, S.: Phys. Rev. Lett. **77**, 4887 (1996)
69. Wodkiewicz, K., Knight, P.L., Buckle, S.J., Barnett, S.M.: Phys. Rev. A **35**, 2567 (1987)
70. Mandel, L.: Phys. Scr. **T12**, 34 (1986)
71. Janszky, J., Vinogradov, A.V.: Phys. Rev. Lett. **64**, 2771 (1990)
72. Buzek, V., Knight, P.L.: Opt. Commun. **81**, 331 (1991)
73. Vidiella-Barranco, A., Buzek, V., Knight, P.L., Lai, W.K.: In: Tombesi, P., Walls, D.F. (eds.) Quantum Measurement in Optics. NATO ASI series. Plenum, New York (1992)
74. Buzek, V., Vidiella-Barranco, A., Knight, P.L.: Phys. Rev. A **45**, 6570 (1992)
75. Schleich, W., Pernigo, M., Kien, F.L.: Phys. Rev. A **44**, 2172 (1991)
76. Buck, B., Sukumar, C.V.: Phys. Lett. A **81**, 132 (1989)
77. Bužek, V., Jex, I.: Quantum Opt. **2**, 147 (1989)
78. Bužek, V.: Phys. Rev. A **39**, 3196 (1989)
79. Obada, A.-S.F., Hessian, H.A.: J. Opt. Soc. Am. B **21**, 1535 (2004)
80. Araki, H., Lieb, E.: Commun. Math. Phys. **18**, 160 (1970)
81. Vidal, G., Werner, R.F.: Phys. Rev. A **65**, 032314 (2002)
82. Bose, S., Fuentes-Guridi, I., Knight, P.L., Vedral, V.: Subsystem purity as an enforcer of entanglement. Phys. Rev. Lett. **87**, 050401 (2001)
83. Bose, S., Fuentes-Guridi, I., Knight, P.L., Vedral, V.: Erratum: Subsystem purity as an enforcer of entanglement [Phys. Rev. Lett. 87, 050401 (2001)]. Phys. Rev. Lett. **87**, 279901 (2001)
84. Scheel, S., Eisert, J., Knight, P.L., Plenio, M.B.: Hot entanglement in a simple dynamical model. quant-ph/207120